Third International Conference on Sustainable Construction Materials and Technologies http://www.claisse.info/Proceedings.htm

The diagnosis of Severely Damaged RC Bridge Piers with Fracture of Steel Bars due to Alkali-Silica Reaction

Akinori KOMATUBARA[1], Kazuyuki TORII[2], Kiyoaki, KAWAUTI[3], Masahiro NOMURA[4]

[1]*Central Nippon expressway Corp. Takayama Maintenance/Customer Service Center, Japan*
[2]*Professor, Dept. of Environmental Design, Kanazawa University, Japan*
[3]*Central Nippon expressway Corp. Kanazawa branch, Japan*
[4]*Central Nippon Highway Engineering Nagoya Corp. Kanazawa branch, Japan*

ABSTRACT

In RC bridge Piers in Toyama Prefecture, Japan, the brittle fracture of steel bars has been found out in the bending of shear steel reinforcements. It was reported that these steel bars were produced by a blast furnace steel maker. In this study, an investigation on the deterioration of steel bars induced by ASR was carried out, based on the measurements of the existing tensile stresses of steel bars and their mechanical and chemical properties. The existing tensile stresses were found to be beyond the yielding point. In the SEM observation near the knot of steel bars, the progress of the brittle fracture was divided into three phases. Because the N content of steel obtained in the chemical composition analysis was 0.014%, it could not be confirmed whether the steel bars were the blast furnace type or the electric furnace type.

Keywords. Alkali-silica reaction, De-icing salts, Fracture of reinforcing steel, Blast furnace steel bar, actual stress of steel bar

1. Introduction

In the Hokuriku district, many cases of fracture of steel bars due to excessive alkali silica reaction (hereinafter ASR) induced expansion have been reported. The main reactive rock class in the Hokuriku district is andesite and the reactive minerals are cristobalite and volcanic glass. For cristobalite there is a pessimum mixing ratio to non-reactive aggregates, whereas pessimum does not exist in the case of volcanic glass. Because the andesite of Hokuriku district contains both minerals, it shows a complex expansion behaviour. On the other hand, most of the cases of fracture of steel bars were observed in RC bridge piers, but cases of fracture of steel in footings and abutments have been also reported. The fracture of reinforcing steel bars in the Hokuriku district is said to be affected by an heavy scattering of de-icing salts, climate conditions such as sunlight and rain, bending and welding pressure, the shape of knots of steel bar which resemble bamboo-like knots and the common use of electric furnace steel bars.

As for the road structures in this investigation, the countermeasures for concrete delamination included the retrofitting of the main structural elements of important intersections. However, fracture of reinforcing steel was observed in the parapets, where the

bridge piers have different heights. Water leakage from the expansion joints has been exposing the parapets to the influence of de-icing salts scattered during the winter season for many years. Therefore, cracks induced by ASR expansion rapidly developed in these past ten years, and other types of deterioration such as reinforcing steel bar corrosion have been also accelerated. The reinforcing steel bars that fractured were shear reinforcement D16 bars and is proved to be reinforcing steel bars produced by a blast furnace maker, from the records at the time of the construction. In this study, the deterioration characteristics of concrete piers affected by fracture of reinforcing steel bars, the petrography of the aggregates and the mechanical properties of concrete cores and reinforcing steel bars collected from the field survey were thoroughly investigated. Furthermore, the authors compared the materials of the reinforcing steel bar removed from the RC Bridge Pier with those of a new electric furnace reinforcing steel bar.

2. The deterioration characteristics of concrete and fracture of reinforcing steel bars in Bridge Piers

The road bridge (hereinafter M bridge) affected by fracture of reinforcing steel is a 2-span PC post-tensioned T girder inaugurated in 1980. Because the span lengths are different, the heights of each girder are different and have a parapet (1,100 mm in width; 1,300mm in height) in the pier. The M bridge is located on the plains near the Toyama city, and only approximately 12km far from the bridge (hereinafter A bridge) of a Case Study of fracture of reinforcing steel that Mr. Daidai and others reported. A lot of microcracks occurred around the concrete aggregates in the A bridge piers and were in such deteriorated condition that were easily broken in pieces by a jackhammer. Therefore, it was believed that similar aggregates from the Jouganji Riverbed might have been used, because both bridges were built before the alkali content regulation was promulgated. The ASR deterioration in the M bridge was discovered in 1993. Some changes of colour and cracking of concrete occurred at first, but delamination of concrete was confirmed in 2008. Fracture of reinforcing steel was confirmed in the bending corners and horizontal surface cracks of 0.5-1.2mm width occurred, as shown in Figure – 1. These fractures occurred on the road shoulder side in 16 different places in total, all at the bending of D16 shear reinforcement bars and distributed @300mm. In addition, the reinforcing steel bar had already corroded and in some, section loss was also confirmed, as shown in Figure – 2. The shape of the knot of the reinforcing steel bars resemble a form of bamboo. On the other hand, the fracture did not occur in the D19 reinforcing steel bars placed in the bridge's vertical axis direction.

3. Results and evaluation of the detailed investigation

A pair of deep penetration cores (φ=55mm; L=1,100 mm) each crossing the parapet from A1 to A2 side was drilled between the fracture of reinforcing steel vicinity (hereinafter, deteriorated part) and the bridge pier centre (hereinafter, sound part) and were used for a detailed concrete property investigation.

3. 1 Rock class composition ratio of course aggregates

We assessed the rock class of aggregate particles with size higher than 5mm observed in core lateral surface (L=200mm) and calculated the composition ratio of the rock, as shown in Figure – 3. River sand and river gravel were used as concrete aggregates. As alkali silica reactive rock types, andesite and rhyolite from volcanic rocks and tuffs were confirmed. In particular, the composition of highly reactive andesite rock was 7%, but this was a small amount if compared with 41% andesite composition ratio in the A bridge. It is reported that

in the Hokuriku district, the severity of ASR increases proportionately to the andesite composition ratio. Therefore, it was assessed that ASR did not progress much in comparison with the A bridge.

3. 2 Observation of ASR degree of deterioration by polarizing microscope

Thin sections were made from the central part of concrete cores and observed by polarizing microscope to confirm the deterioration condition due to ASR. Figure – 4 shows the reaction of an andesite particle from river sand. A 0.1mm crack developed from the sand particle and progressed into the cement paste, was filled with an unstable and amorphous form of gel. Figure – 5 shows the reaction stage of an andesite particle from river gravel aggregate. Large cracks of around 1mm width occurred in 20mm diameter andesite particles and penetrated into the cement paste. Similarly, we confirmed the presence of an unstable and amorphous form of gel. In addition, the gel which filled the air voids was also observed around the andesite particles and judging from the thin section observation, the stage ASR deterioration had considerably progressed. The reaction degree of the andesite particle was approximately similar to the one observed in the A bridge. The simultaneous reaction of river sand and river gravel could be an indication that aggregates from the Jouganji riverbed were used in the concrete mix.

3. 3 Results of chloride and alkali content measurements

Using the concrete cores drilled from the deteriorated part, the chloride ion concentration that penetrated from the parapet surface was measured in accordance to JIS A 1154, a method based on nitric acid extraction. The results are shown in Figure – 6. Because the parapet's A1 side was rightly under an expansion joint, it was affected by de-icing salts scattered during the winter season and the penetration of highly-concentrated chloride ions was confirmed. The value exceeded the 1.2 kg/m3 threshold for steel corrosion occurrence, and was higher than the chloride ion concentration observed in the A bridge. On the other hand, there was little chloride ion penetration on the A2 side. However, fracture of reinforcing steel bar was observed in the bending sections of A2 side, and it is believed that this fact was unrelated to the chloride ion penetration.

The quantity of alkali equivalent (Na2Oeq.) in concrete was measured from concrete cores drilled to around 50cm in depth from the parapet's surface, which was not affected by de-icing salts. The measurements were based on extraction of warm water mixed with concrete powder at 40 degrees Celsius. The quantity of alkali equivalent was 2.9-3.4 kg/m3, and was approximately the same level of 2.6-2.9 kg/m3 observed in the A bridge.

3. 4 Result of accelerated ASR test

Because the M bridge was affected by de-icing salts, we evaluated the residual expansibility of concrete in accordance with the Danish mortar bar method (temperature 50 degrees Celsius; saturated NaCl solution). One part of the concrete core was used in this test and the results are shown in Figure – 7. In the sections affected by de-icing salts, the residual expansion ratio was less than 0.05% after 91 days testing period, and it was judged that ASR was in recession. On the other hand, the expansion ratio increased in the sound concrete part, which was not affected by de-icing salts, during the same testing period. The expansion ratio was at the same level of A bridge, and the similarity of the residual expansion of concrete was also observed. The ASR progress in the different parts of the bridge pier (shoulder and center of the parapet) turned out different and was greatly affected by influence of sunlight, frequency of wet-dry cycles and exposure to de-icing salts.

3. 5 Result of compressive strength and static elastic modulus of concrete cores

The compressive strength and static elastic modulus tests were carried out with a portion of the concrete core and the test results are shown in Figure – 8. In addition, the ratio of the static elastic modulus / compressive strength of the concrete core is presented in the vertical axis. The compressive strength of 20N/mm2 was less than the design strength of 24N/mm2, and it was noted that the static elastic modulus also decreased. The concrete cores drilled from the damaged parts were all plotted below the curve of "sound concrete" recommended by the Japan Society of Civil Engineers and Technical Handbook of the Japan Roads and Bridges.

3. 6 Field test results of reinforcing steel bar stress in RC bridge piers

The reinforcing steel bars were exposed to estimate the actual stress level and the measurements were carried out in accordance with the single fracture method. The setting up of the strain gauges and the cutting position of the steel bar are shown in Figure – 9. The investigation targeted the shear reinforcement and we compared the stress in fractured steel bars with those without fracture. The strain of fractured reinforcing steel bars was approximately 1,800 μ (actual stress 370N/mm2) and approximately 1,400 μ (actual stress 290N/mm2) in non-fractured steel bars. In addition, this data was corrected for temperature stress that occurred at the time of cutting the steel bar with a grinder, by attaching a thermocouple to the strain gauges. From the record at the time of the construction of M bridge, the type of reinforcing steel bars used was SD295A and it was observed that the stress levels that developed due to excessive ASR expansion exceeded the steel yielding point.

3. 7 Material properties of reinforcing steel bars

(1) Knot shape of the reinforcing steel bars

A D16 reinforcing steel bar removed from the structure was subjected to a C cut and L cut, and the knot shapes were examined. The results are shown in Figure – 10. The distance between the knots was 9.7mm, the height of the knot was 1.2-1.3mm, the angle between the knot and the axis was 45 degrees, overall in conformance to JIS G 3112 specifications.

(2) Tensile strength of reinforcing steel bars

In order to assess the mechanical properties of fractured reinforcing steel bars, three D16 bars and one D19 bar were removed from the structure and subjected to tensile strength tests. The test results are shown in Table – 1. The yielding point and the tensile strength satisfied the JIS G 3112 specifications. However, the D19 showed a smaller strength than the D16 bars and it is believed that this difference could be related to a possible damage to the steel bar during the removal process from the structure.

(3) Chemical composition of reinforcing steel bars

The chemical composition analysis of D16 and D19 steel bars was carried out with different methods. For C (carbon) and S (sulphur), the infrared absorption method (JIS G 12113) was used, N (nitrogen) was analyzed by nitrogen content method in iron and steel (JIS G 12283 (4)), and other elements by spark electric fluorescence spectrometry analysis (JIS G 1253). The test results are shown in Table – 2. The general chemical composition of electric furnace and blast furnace reinforcing steel bars are shown in this table. The analysis of the chemical

composition satisfied the JIS G 3112 specifications, but the composition of Si, Mn, Cu, Al and N turned out to be similar to the composition of electric furnace steel bars. Especially, because the high nitrogen content, some loss of toughness occur and it is believed that, when bending the reinforcing steel bar, it is affected by a permanent strain and cracks.

(4) The measurement of the bending radius and crack assessment

After getting samples of bent D16 steel bars and have cleaned the surface, a digital microscope was used to determine the bending radius and assess the existence of microcracks. The steel bar used in the experiments is shown in the Figure – 11. The interior bending radius was 17mm, which was approximately 1.1 times the reinforcing steel bar diameter and did not satisfy the 2.0 times design steel bar bending radius. The crack formation in the reinforcing steel bar is shown in Figure – 12. On the lateral side of the bending, cracks developed along the rolling direction. In addition, cracks parallel to the R part of the knot and cracks parallel to the rolling direction were confirmed in the internal part of the bending. On the other hand, cracks did not occur on the external side of the bending. As for the microcrack formation in the reinforcing steel bars, it is believed that a reduction of steel toughness due to high N content and the small bending radius were the main causes.

(5) SEM observation of the fracture surface of the reinforcing steel bars

After cleaning the fractured surface of bent reinforcing steel bars, it was observed by a scanning electronic microscope (SEM). A fractured surface of reinforcing steel bar is shown in Figure – 13, the SEM image of a crack starting point and the crack propagation part are shown in Figure – 14 and Figure – 15, respectively. The fracture starting point is located in the interior side of the bending and it further propagates in three distinct phases toward the external side of the bending. In addition, both the starting part and the propagation part presented a brittle-type of fracture. As shown in Figure – 13, it is believed that the brittle fracture occurred from the starting point, spread up to the dotted line and stopped. Then, the fracture propagation (divided into three phases), occurred from the dotted line onwards. Such fracture behaviour was firstly suggested in a report by Tarui.

4. Conclusions

Fracture of reinforcing steel due to excessive ASR expansion was observed in structures using reinforcing steel bars from a blast furnace maker. Because of the high toughness of reinforcing steel made conventionally in blast furnace makers, it was believed that the fracture of steel was unlikely to occur as result of ASR-induced expansion. The main conclusions of this investigation are summarized below:

(1) The fracture of D16 reinforcing steel bar was a result of shear and bending, combined with a knot shape resembling a bamboo-like knot.

(2) In the points where fracture of reinforcing steel was observed, about 1mm width horizontal cracks occurred on the concrete surface due to excessive ASR-induced expansion.

(3) Due to cracks caused by ASR expansion and loss of concrete confinement, the concrete compressive strength fell to 20N/mm2 from a standard design strength of 24N/mm2.

(4) The fracture of reinforcing steel was largely affected by water and de-icing salt leakage from the expansion joints, leading to steel corrosion and section loss.

(5) The andesite particles in the river sand and river gravel, together caused an intense ASR reaction in concrete. In addition, the ASR gel filled the cracks in cement paste, and gel spots were observed by polarizing microscope.

(6) The strain observed in D16 reinforcing steel bars of RC bridge piers by single-fracture method was 1,800 μ. As a result, the estimated stress generated in the steel members was 370KN/mm2, which exceeded the yielding point of SD295A type reinforcing steel bars.

(7) From the materials test result collected on site, the yielding point of reinforcing steel bars was 370N/mm2. However, because the 0.014% N (nitrogen) content in chemical composition was considered high, this blast furnace steel revealed a chemical composition similar to an electric furnace steel bar.

(8) The relationship between the bending radius and the diameter of the reinforcing steel bar (R/D) was 1.1, and this value did not satisfy the design curvature of 2.0. In addition, cracks occurred along the knot and also on the rolling direction of the steel bending segments.

(9) SEM observation of fractured reinforcing steel surface revealed that cracks occurred at the time of bending propagated in a brittle-like way in three distinct phases.

(10) The main causes of fracture of reinforcing steel are believed to be the loss of toughness due to high N (nitrogen) content, small bending radius that led to crack formation and excessive ASR-induced expansion due to the influence of de-icing salts scattered during the winter season.

REFERENCES

Kazuyuki Torii (2010). The Characteristic Feature of Fracture of Steel Reinforcement in ASR-Deteriorated Concrete Structures, Zairyo-to-kankyo (59/4), pp.117-120. (in Japanese).

Masahiro Nomura, Akinori Komatsubara, Masami Kuroyanagi, Kazuyuki Torii (2011). Evaluation of the Residual Expansivity of Cores due to Alkali-Silica Reaction in Hokuriku District, Japan, Concrete Research and Technology (33/1), pp953-958. (in Japanese).

Masahiro Nomura, Akinori Komatsubara, Tomoshi Ushiya, Kazuyuki Torii (2010). Verification of the Evaluation of the Residual Expansivity of cores from ASR-Affected Structures, Concrete Research and Technology (32/1), pp965-970. (in Japanese).

Takeshi Daidai, Kazuyuki Torii (2008). A Proposal for Rehabilitation of ASR-affected Bridge Piers with Fractured Steel Bars, Proceedings of the 13th ICAAR, pp42-49.

Toshimi Tarui, Kazuyuki Torii (2010). Fracture Mechanism of Steel Bar by Alkali Silica Reaction, Zairyo-to-kankyo (59/4), pp.143-150. (in Japanese).

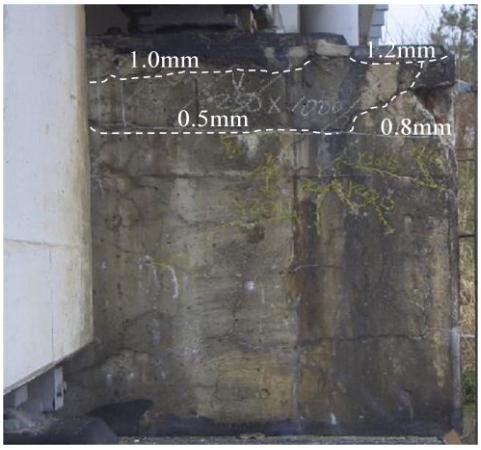

Figure 1. Parapet affected by fracture of reinforcing steel bar

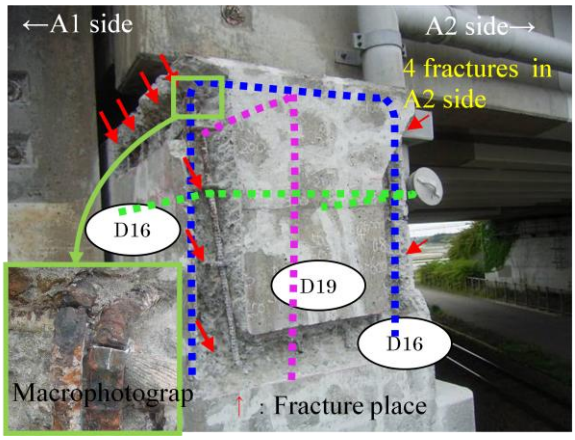

Figure 2. Places and situation of fractures

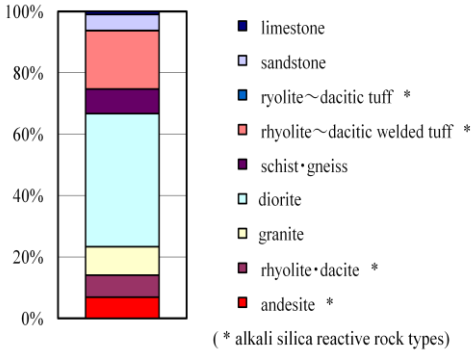

Figure 3. Rock class composition ratio of course aggregates

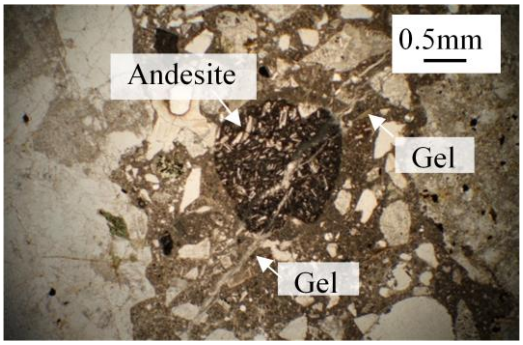

Figure 4. Reaction of an andesite particle from river sand (open nicol)

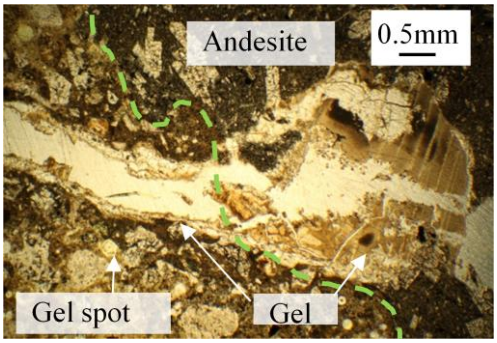

Figure 5. Reaction of an andesite particle from river gravel aggregate (open nicol)

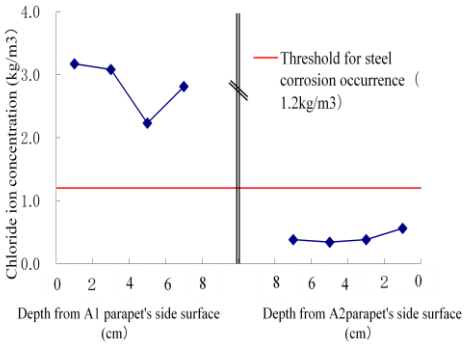

Figure 6. Result of chloride content measurements

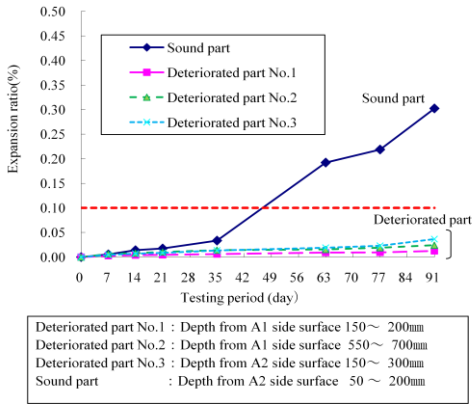

Figure 7. Result of accelerated ASR test with Danish mortar bar method

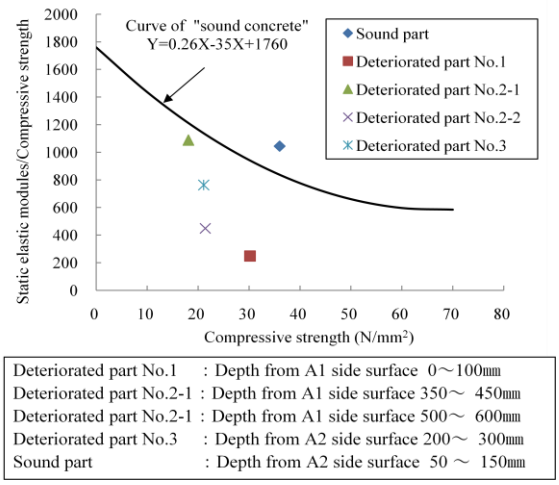

Figure 8. Relationship between ratio of static elastic modules/compressive strength and compressive strength

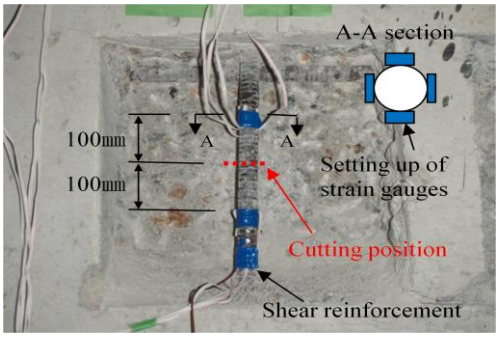

Figure 9. Field test of reinforcing stress with single fracture method

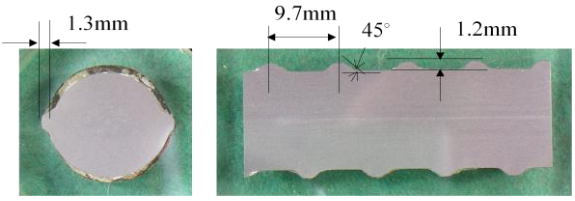

Figure 10. Knot shape of reinforcing steel bars(D16)

Figure 11. Steel bar used in measurement of bending radius (D16)

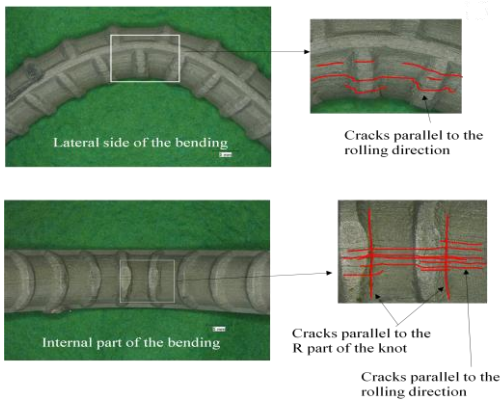

Figure 12. Crack formation in the reinforcing steel bar

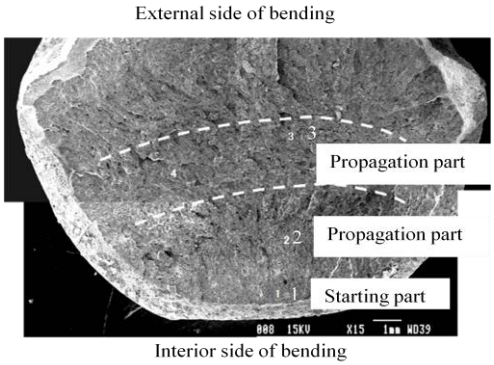

Figure 13. Fracture surface by SEM observation

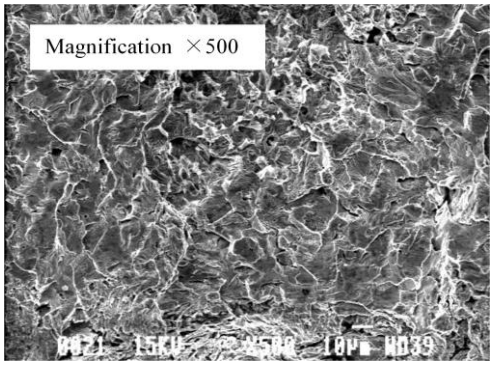

Figure 14. SEM image of a crack starting point

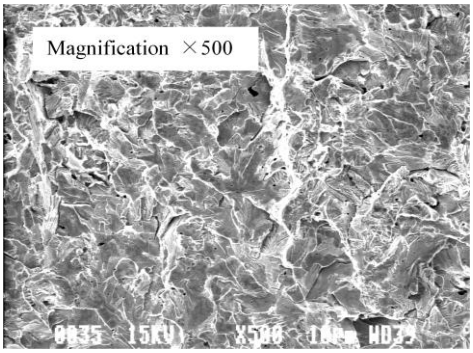

Figure 15. SEM image of a crack propagation part

Table 1. Results of tensile strength tests

Size	Yielding point	Tensile strength
D16	373～381N/ mm^2	555～555N/ mm^2
D19	323N/ mm^2	471N/mm^2

Table 2. Results of chemical composition analysis of reinforcing steel bars

Element	C	Si	Mn	P	S	Cr	Mo	Ni	Cu	Al	N
D16	0.27	0.16	0.84	0.035	0.018	0.11	0.010	0.071	0.20	<0.002	0.0135
D19	0.23	0.13	0.90	0.030	0.024	0.20	0.014	0.062	0.18	<0.002	0.0114
Electric furnace	0.25	0.20	0.97	0.023	0.025	0.19	0.02	0.10	0.19	0.002	0.0116
Blast furnace	0.22	0.33	1.40	0.027	0.021	0.06	0.01	0.02	0.06	0.007	0.0048
JIS G 3112 SD295A	—	—	—	0.05<	0.05<	—	—	—	—	—	—